Published by :
http://www.ijert.org

International Journal of Engineering Research & Technology (IJERT)
ISSN: 2278-0181
Vol. 14 Issue 02, February-2025

Numerical Study of Flow and Aerodynamic Forces Generated by a Cropped Delta Flying Wing

Authors:
Jaya Kushwaha And Gnanvitha Kosaraju
(Amity Institute of Technology, Amity University Noida, Uttar Pradesh)

Under the guidance of
Dr R. S. Tarnacha
(Amity Institute of Technology, Amity University Noida,
Uttar Pradesh, Consultant Tata Technologies Ltd.)

ABSTRACT

Many supersonic aircraft utilize delta wing designs. Since the 1950s, delta wings have been extensively researched, revealing that at high angles of attack, they generate two significant counter-rotating leading-edge vortices. These vortices enhance lift and increase the wing's stall angle. At elevated Mach numbers, compressibility effects promote leading edge separation and amplify the strength of primary vortices. The formation of shock waves due to high-speed airflow over the delta wing results in notable alterations in flow behavior. While supersonic jets typically feature delta wing configurations, they often operate at subsonic speeds, leading to a focus on both subsonic and supersonic flight regimes in this study. This study involves numerical simulations of the flow over a cropped delta wing at Mach numbers ranging from 0.29 to 1.75 and angles of attack from 0Â° to 35Â°, utilizing a computational model. Steady-state computations based on Reynolds Averaged Navier-Stokes (RANS) equations were performed, employing the K epsilon turbulence model for its computational efficiency and effectiveness in simulating external flows. Given the involvement of supersonic conditions, the model accounted for compressibility. The findings indicate a sudden alteration in flow characteristics as Mach number increases. Near the delta wing surface beneath the primary vortex, the flow becomes entirely supersonic, with shock waves forming at Mach 1.75, complicating the flow fields. At high Mach numbers, the enhanced strength of the primary vortex inhibits the development of inner separation, leading to the disappearance of the secondary vortex. Additionally, the results support the concept of vortex breakdown, which contributes to the nonlinear behavior of flow characteristics over the wing as the Mach number rises. The Pressure contours, pressure distribution plots and streamlines are observed along chordwise and spanwise location.

INTRODUCTION

The cropped delta wing design is utilized in many contemporary high-speed fighter jets, such as the HAL Tejas (Light Combat Aircraft). This configuration enhances stability and maneuverability, which are crucial for fighter performance. Additionally, delta wings are known for their reduced supersonic drag, and using sharp or thin leading edges can further optimize this feature. The pressure difference across the wing causes airflow over the lower surface to move toward the upper surface, leading to flow separation at the leading edge. This results in the formation of two counter-rotating leading-edge vortices (LEVs) that travel downstream, as illustrated in Figure 1. The vortices generate a flow field that drastically modifies the wing's aerodynamic properties, rendering them highly unpredictable. As the angle of attack rises, the behavior of the LEVs alters, and they may experience "breakdown" or "bursting." This incident may provide unstable aerodynamic loads on the wing, perhaps leading to buffeting. Therefore, understanding vortex breakdown is critical for aircraft designers. This report will focus on a study of the cropped delta wing for which NACA 0012 airfoil will be used for the Tejas aircraft. The specified airfoil is selected because it has zero camber and plenty of data is available for the validation of results

Published by :
http://www.ijert.org

International Journal of Engineering Research & Technology (IJERT)
ISSN: 2278-0181
Vol. 14 Issue 02, February-2025

CFD MODELLING

The flow field was then produced around the wing in a C-section configuration. The radius of the half circle in front of the airfoil was taken as 15 metres long, whereas the length of the area behind the wing was 30 m for the better visualization of flow downstream of the wing. Length of the root airfoil chord is 7.63 m , middle chord is 5.73 m, tip chord is 0.93 m. The goal is to model the flow through the designated area while cutting out the wing surface from the flow domain, allowing it to function as a wall over which the free stream moves.

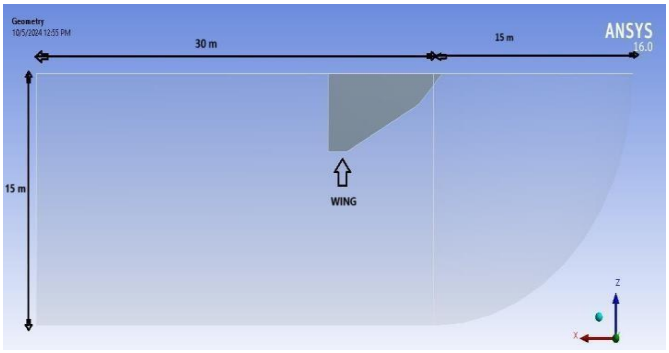

Figure 1: Computational domain

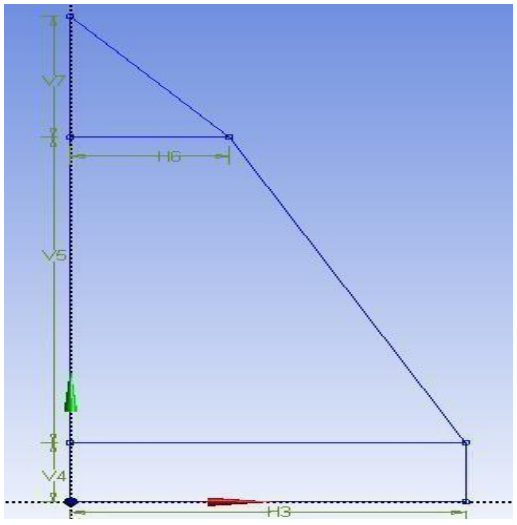

Figure 2: CFD modelling of flow domain

Dimensions: 5	
H3	4.1 m
H6	1.65 m
V4	0.93 m
V5	4.8 m
V7	1.9 m

MESHING

Global mesh controls influence the entire grid, whilst local meshing settings, available from the mesh control menu has been applied to individual features. For this investigation, the ANSYS Mesher was used to build a mesh that is compatible with the ANSYS Fluent. The flow field is considered to be symmetric along the center line of the wing. As a result, the computational domain only extends to half of the wing.

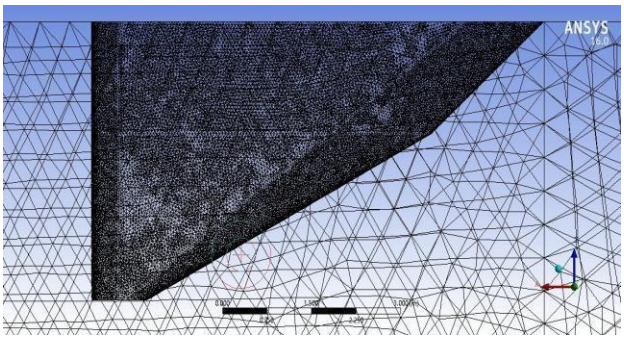

Figure 3: Mesh geometry of the symmetric one-half of the wing used for analyzing.

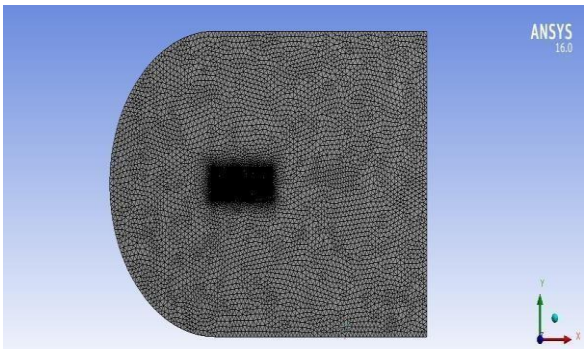

Figure 4: Meshed geometry of the whole domain used for analysis. A body of influence was created around the 3-D wing to obtain denser mesh in its proximity as seen the above figure

Published by :
http://www.ijert.org

International Journal of Engineering Research & Technology (IJERT)
ISSN: 2278-0181
Vol. 14 Issue 02, February-2025

SETUP FOR SOLVER

ANSYS Fluent uses the finite volume method to solve the fluid dynamics governing equations. The first step in CFD modeling is to create the geometry of a 3-D wing, which is done using NACA 0012 airfoil data from (1) into ANSYS Design Modeler. Following that, mesh settings and configurations are set up. Next, the solver settings and preferences are selected along with the boundary and inflow conditions. For the flow simulation, the standard k-e, standard wall function turbulence model is chosen, along with a pressure-based algorithm. Finally, the post- processing stage presents pressure and velocity contours, pressure distribution plots, streamlines etc.

Once the meshing is completed, the next phase involves setting up the conditions and selecting the appropriate solver options. For this analysis, a pressure-based model has been chosen for subsonic case. Historically, this pressure-based method was designed for low-speed incompressible flows. The momentum equations are used to calculate the velocity field. In the pressure-based method, the pressure field is calculated by solving a pressure or pressure correction equation derived from the continuity and momentum equations.

For the solver, the FLUENT solver is utilized alongside a pressure-based model for subsonic case where the velocity formulation is set to 100 m/s. The simulation is conducted under steady-state conditions, meaning that the flow remains unchanged after the initial boundary conditions are established. The objective is to analyze the full Navier-Stokes equations, which requires accounting for viscosity effects. As a result, the turbulence model is configured as the k-e standard wall function two-equation model. The fluid used in the flow analysis is air, but to accommodate compressibility at higher Mach numbers, the density is calculated using the ideal gas law for the supersonic case while for subsonic density is considered as constant and at sea level. For boundary conditions, a velocity inlet and a pressure outlet is selected, As a result, the wing face is defined as a wall with no- slip wall boundary, which indicates that the velocity at the wall's face is zero. Also symmetry is defined as symmetry.

The reference values for calculating lift and drag forces, are derived from the inlet. In this study, the area of interest is simply the chord wing area which is given as 38.36 m^2 while the mean aerodynamic chord has been found as 5.52 m.

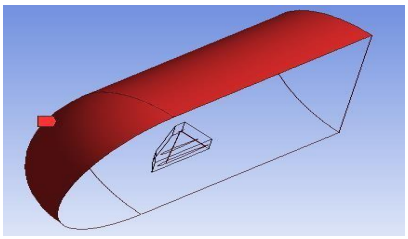

Figure 5: Inlet

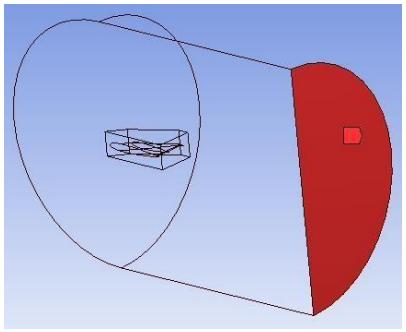

Figure 6: Outlet

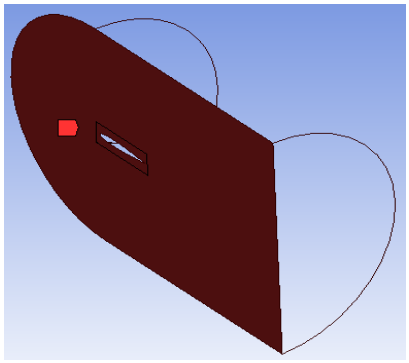

Figure 7: Symmetry

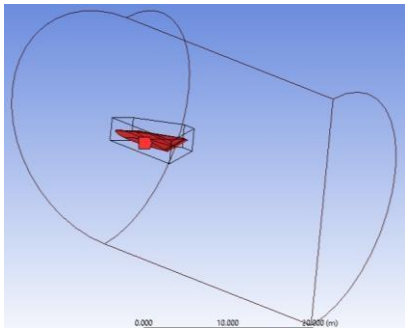

Figure 8: Wing

After successful solution was obtained, the results obtained in post-processing are described in the following paragraphs.

Published by :
http://www.ijert.org

International Journal of Engineering Research & Technology (IJERT)
ISSN: 2278-0181
Vol. 14 Issue 02, February-2025

POST PROCESSING

Pressure distribution plots

The Figures 9-16 shows the resulting pressure distribution along the chordwise length. The conditions of the simulation are M = 0.29 at 0°,5°,10°,15°,20°,25°,30° angles of attack . The difference between the plotted curves gives idea of lift generated in each case. It can easily be observed that there is low pressure on the upper surface while high pressure on the bottom surface as evident from the figures.

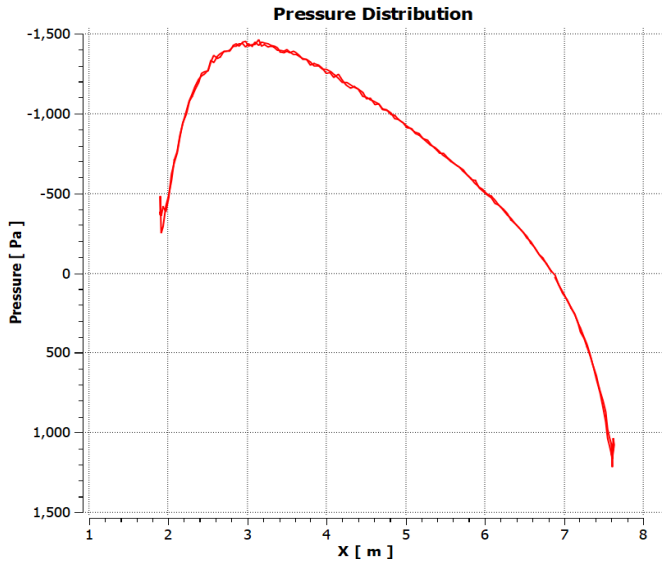

Fig 9 α= 0°

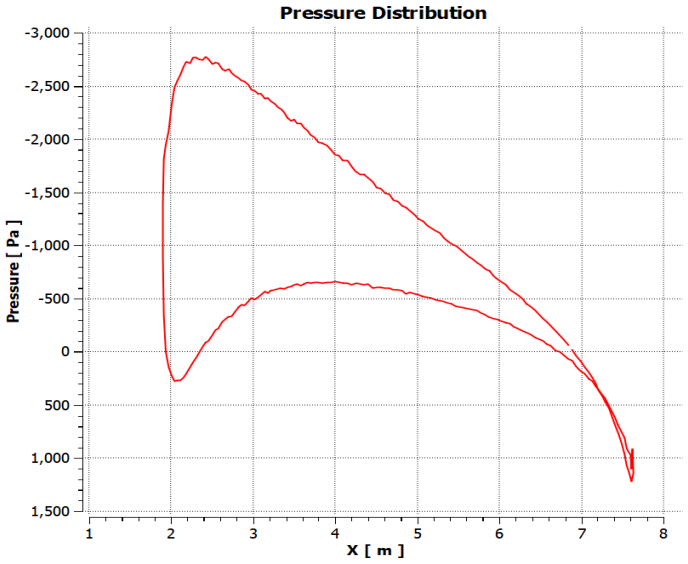

Fig 10 α= 5°

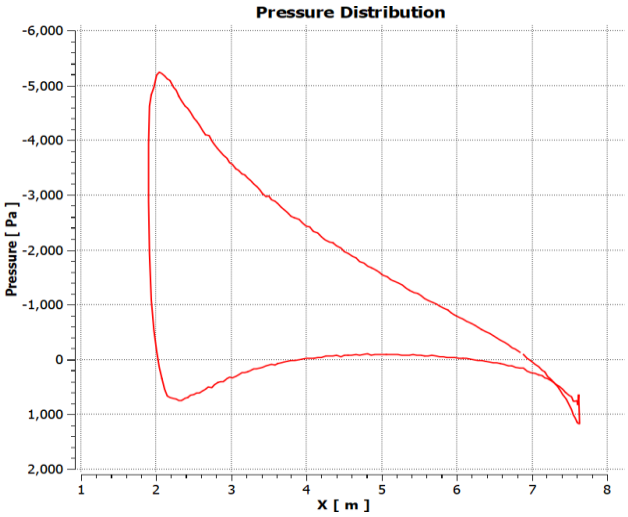

Fig 11 α= 10°

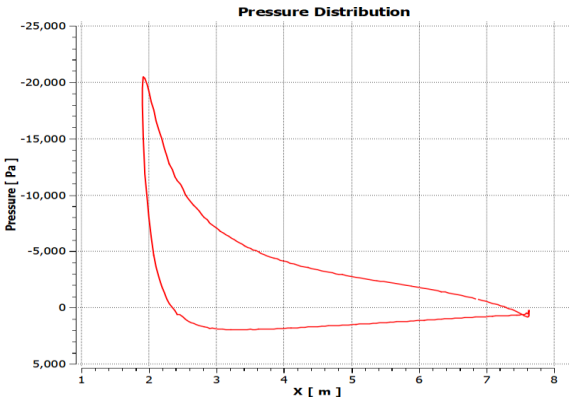

Fig 12 α= 15°

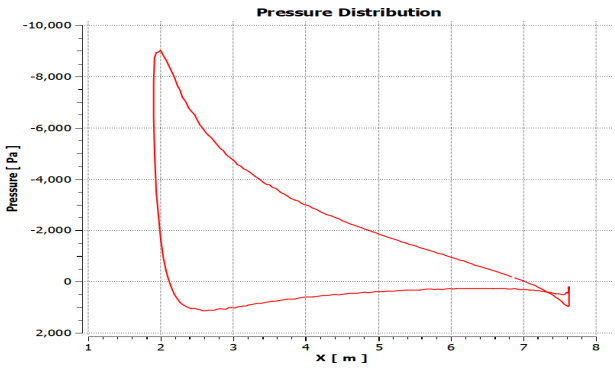

Fig 13 α= 20°

Published by :
http://www.ijert.org

International Journal of Engineering Research & Technology (IJERT)
ISSN: 2278-0181
Vol. 14 Issue 02, February-2025

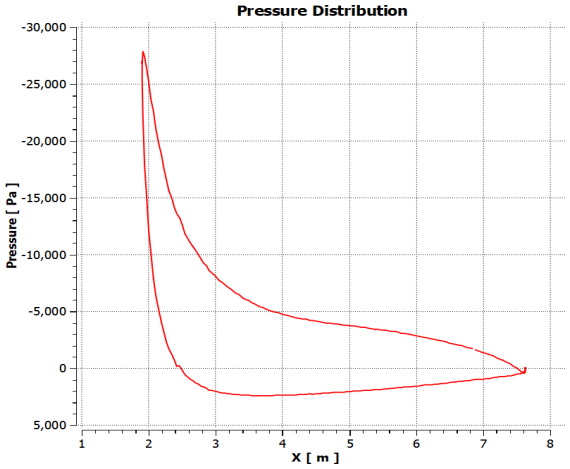

Fig 14 α= 25°

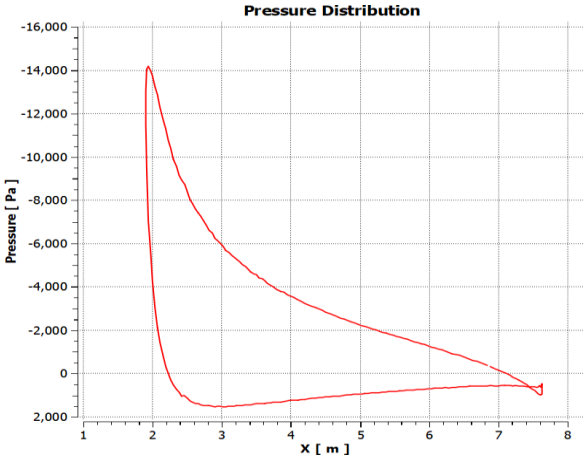

Fig 15 α= 30°

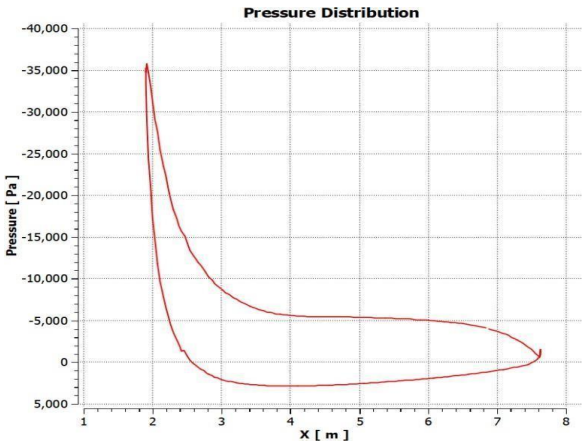

Fig 16 α= 35°

PRESSURE CONTOURS

On a delta wing with NACA 0012 airfoil, the stagnation point, where fluid velocity is zero, shifts significantly as the AOA increases from 0 to 35. At 0, the stagnation point is typically located at or near the leading end apex. As the AOA increases, the stagnation point gradually moves toward the upper surface of the wing. This movement is influenced by the increasing pressure difference between the upper and lower surfaces generates lift. However beyond a certain AOA (around 20- 30), the foil separation on the lower surface becomes more pronounced, potentially limiting further movement of the stagnation point. This general trend provides a basic understanding of stagnation point behavior on a delta wing.

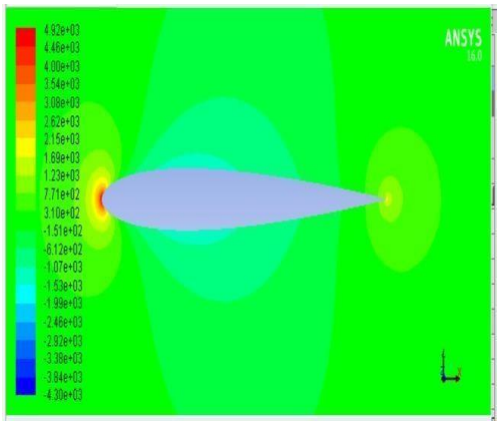

Fig 17: α= 0°

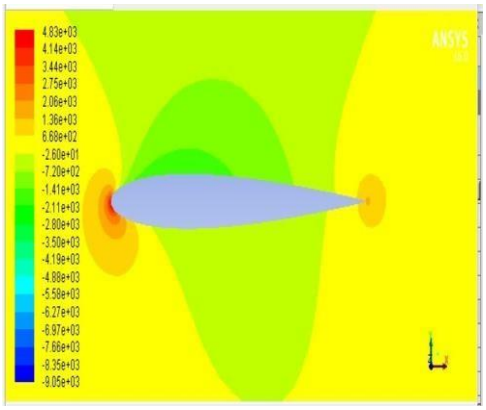

Fig 18: α= 5°

Published by :
http://www.ijert.org

International Journal of Engineering Research & Technology (IJERT)
ISSN: 2278-0181
Vol. 14 Issue 02, February-2025

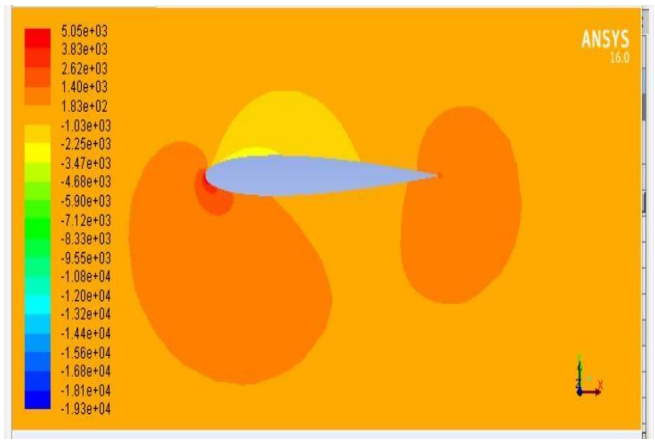

Fig 19: α= 10°

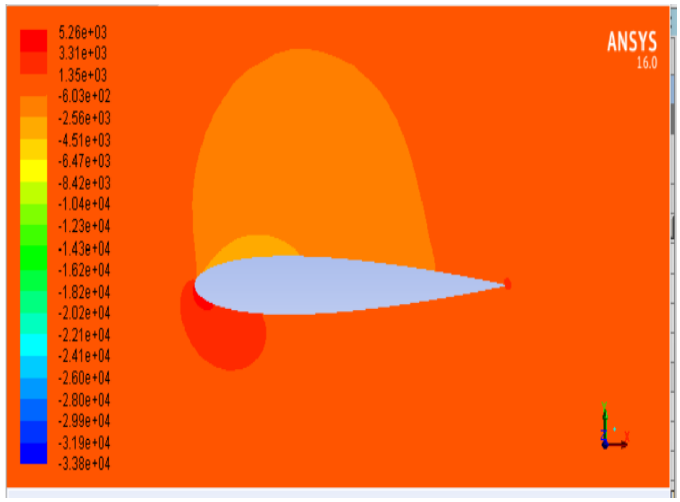

Fig 20: α= 15°

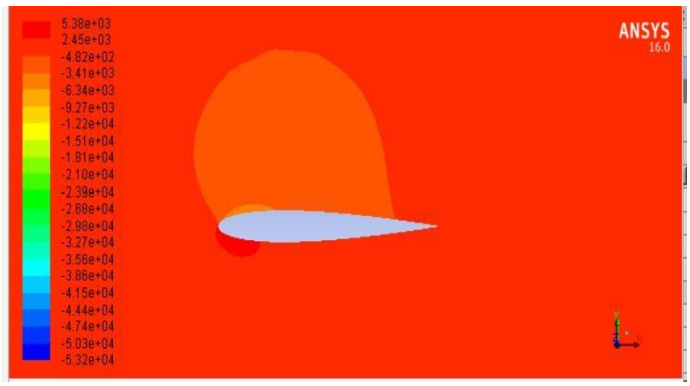

Fig 21: α= 20°

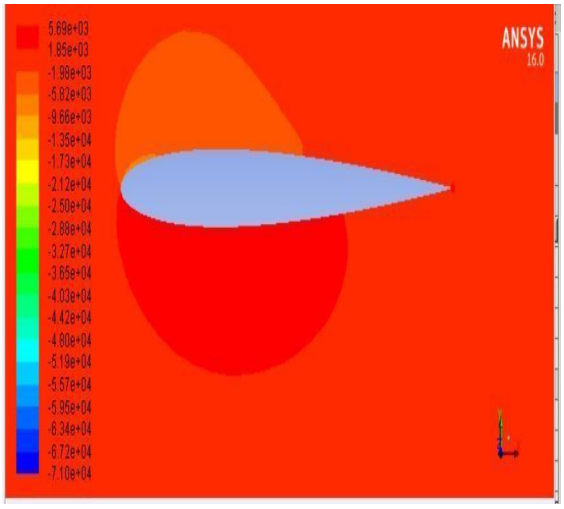

Fig 22: α=30°

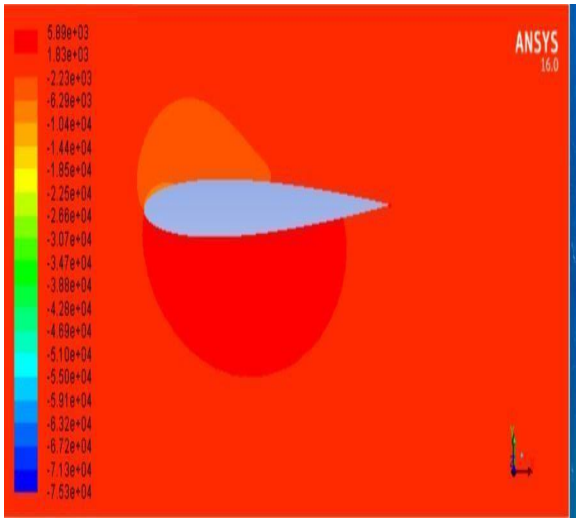

Fig 23: α= 35°

Published by :
http://www.ijert.org

International Journal of Engineering Research & Technology (IJERT)
ISSN: 2278-0181
Vol. 14 Issue 02, February-2025

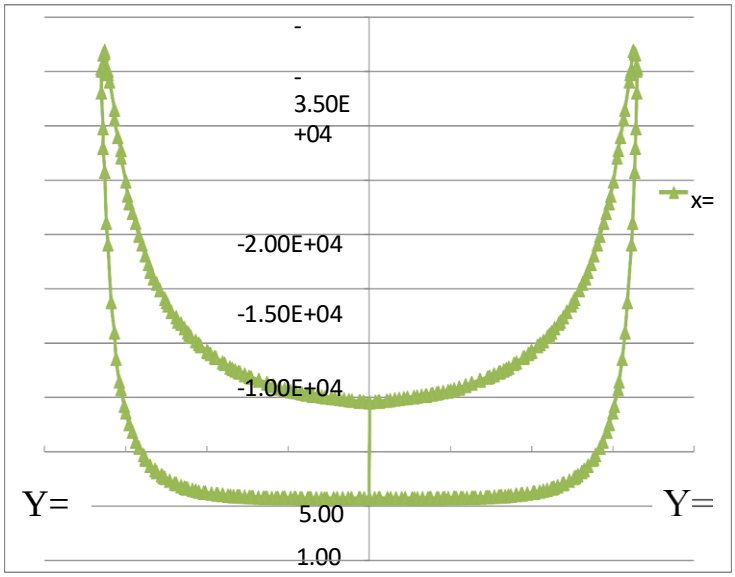

Fig 24: Plot of spanwise pressure distribution across the wing from -b/2 to +b/2 at axial distance x=1.65 m from the leading edge of the root chord.

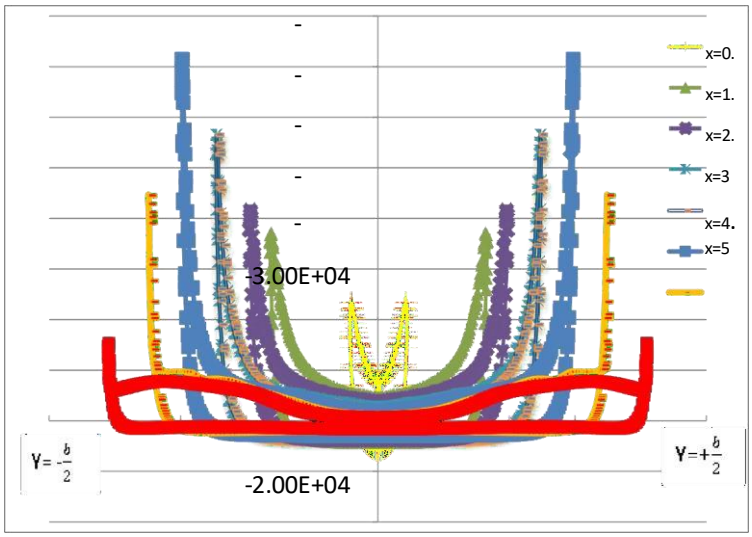

Fig 25: Plot of spanwise pressure distribution across the wing from -b/2 to +b/2 at different axial distances.

Variation of lift coefficient and drag coefficient with angle of attack

Lift and drag coefficient of NACA 0012 airfoil is compared with the data of cropped delta wing which uses the same airfoil at different angles of attack.

Table 1 : C_L vs α

AOA	C_L(ANSYS)	C_L(Theory)
0	0.000022	0.00000
2.5	0.046870	0.26550
5	0.093939	0.62750
10	0.188070	1.04170
15	0.282220	1.23270
19.25	0.370710	
20	0.386920	
25	0.485140	
30	0.568450	
35	0.628780	

Published by :
http://www.ijert.org

International Journal of Engineering Research & Technology (IJERT)
ISSN: 2278-0181
Vol. 14 Issue 02, February-2025

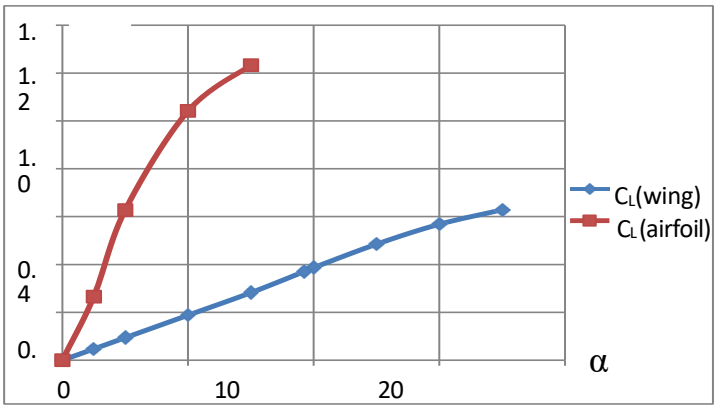

Fig 26 : C_L vs α

Table 2 : C_D vs α

AOA	C_D(ANSYS)	C_D(Theory)
0	0.003126	0.00618
2.5	0.003989	0.00737
5	0.006640	0.00847
10	0.017456	0.01951
15	0.036286	0.04811
19.25	0.062153	
20	0.067884	
25	0.113630	
30	0.175150	
35	0.248490	

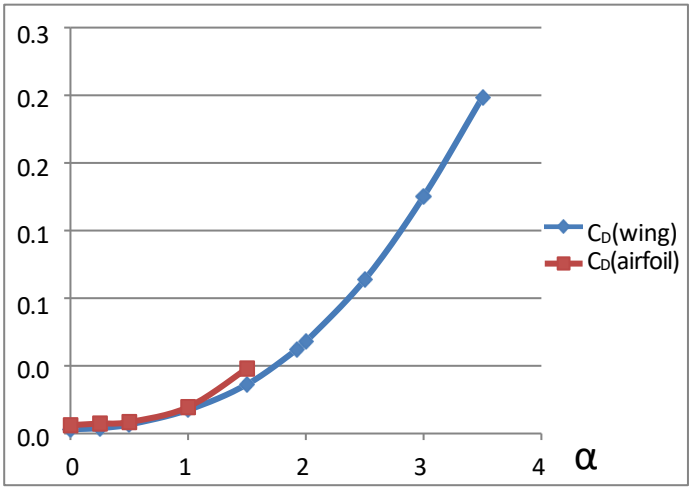

Fig 27 : C_D vs α

STREAMLINES

Cropped delta wings, distinguished by their shortened tips, have unique aerodynamic characteristics that are particularly important in subsonic flight. Observing the behavior of streamlines around these wings at various angles of attack (AoA) provides critical insights into their performance and flow behavior. In figure streamlines are plotted at different angle of attack.

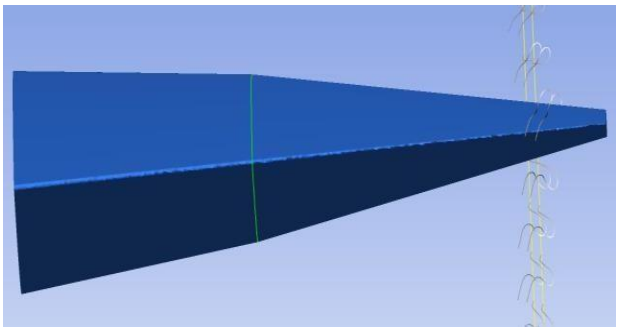

Fig 28: Streamlines at α=0°

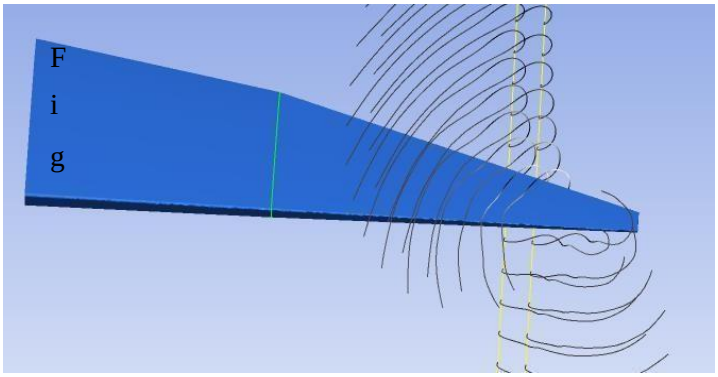

Fig 29: Streamlines at α=5°

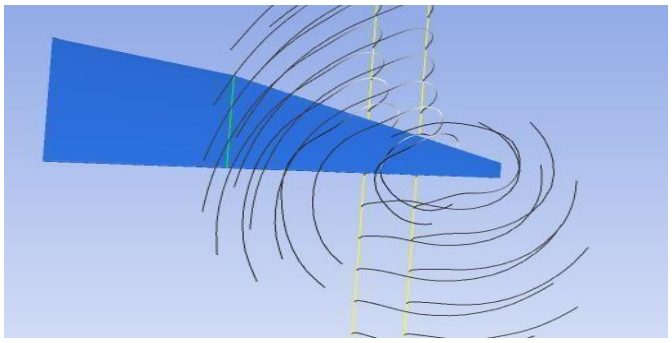

Fig 30: Streamlines at α=10°

Published by :
http://www.ijert.org

International Journal of Engineering Research & Technology (IJERT)
ISSN: 2278-0181
Vol. 14 Issue 02, February-2025

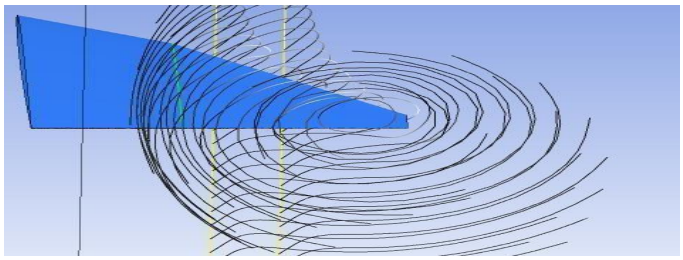

Fig 31: Streamlines around the wing tip at α=15°

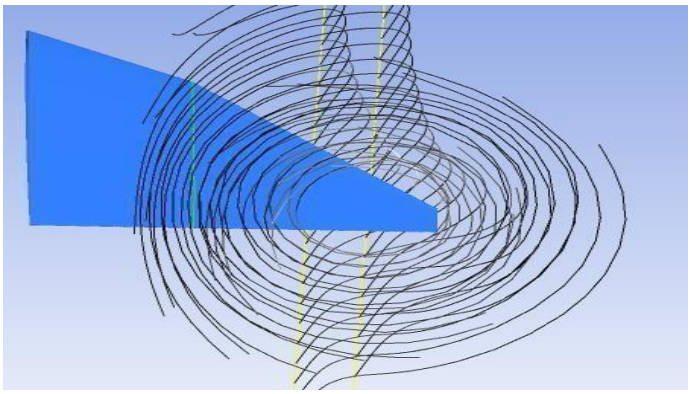

Fig 32: Streamlines around the wing tip at α=20°

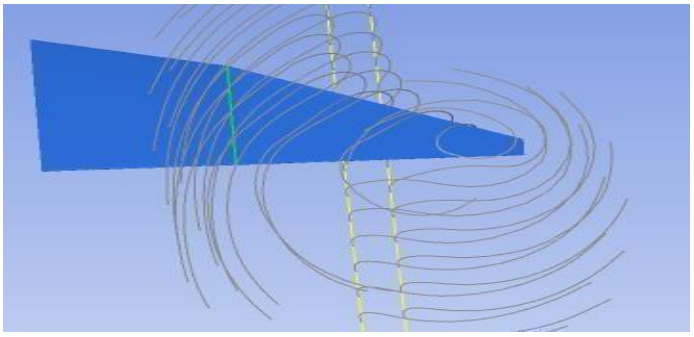

Fig 33: Streamlines around the wing tip at α=25°

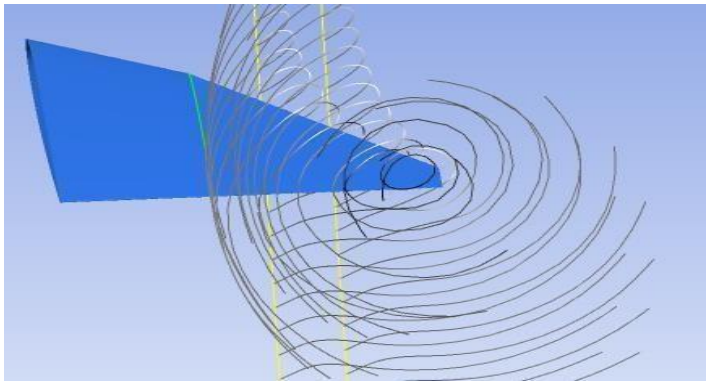

Fig 34: Streamlines around the wing tip at α=30°

PATHLINES

In a steady flow, streamlines, streaklines, and pathlines are the same. Here in this figure surface pathlines using oil-paint selection are plotted for 35° angle of attack to show the vortex formation in the vicinity of leading edge.

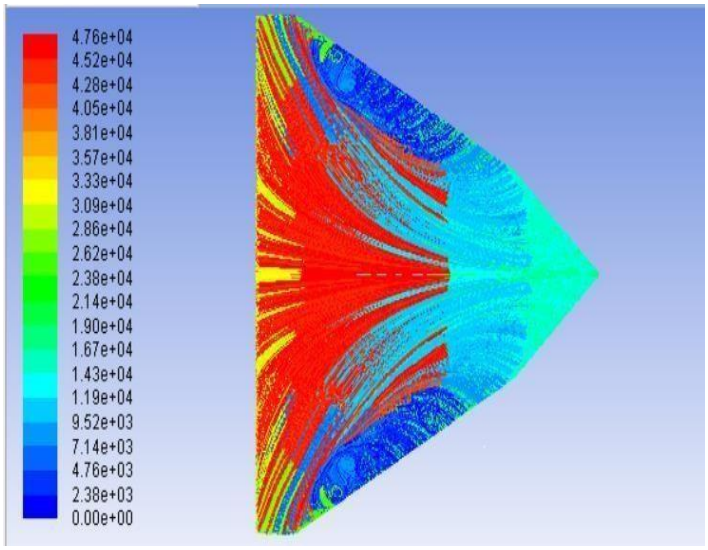

Fig 35: Pathlines on upper surface of delta wing at α=35°

3d view of pressure distribution

In a parallel study a similar 3-D wing was created using NACA64206 airfoil and the spanwise pressure distribution as surface plots at different x-distances from the leading edge of root chord were generated for upper and lower surfaces. These are shown in Figs. 35 and 36.

Fig 36: On upper surface

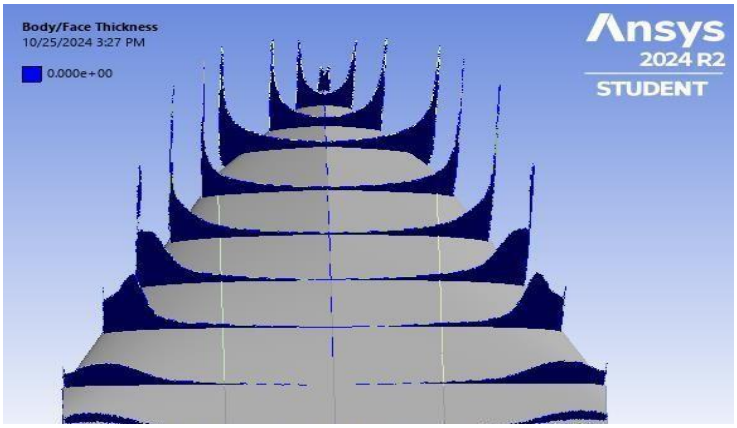

Published by :
http://www.ijert.org

International Journal of Engineering Research & Technology (IJERT)
ISSN: 2278-0181
Vol. 14 Issue 02, February-2025

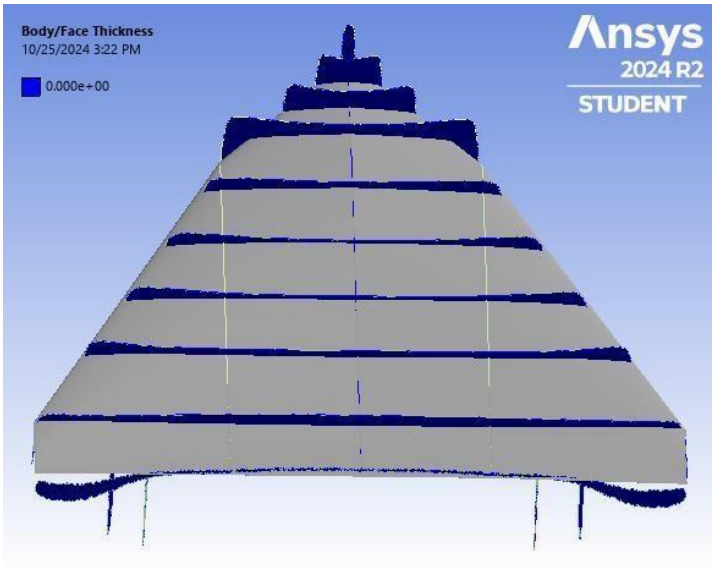

Fig 37: On lower surface

VADLIDATION

In order to validate the above procedure followed in this study, CFD analysis was carried out for flow over airfoil NACA0012. The results were with the data available in website airfoiltoolls.com and found to match reasonably well as shown in Figs 37 and 38. The Lift Coefficient in 3D analysis was found to be less than the 2D airfoil's quoted value in the literature, depicting the complexity of actual wing airflow. The model also considered elements not prominent in 2D simulations, such as flow separation and vortex dynamics. The Drag Coefficient was also examined, and the results were cross-checked against online data available on website airfoiltools.com. The values followed similar trend to the lift coefficient indicating that the trend would be followed for higher angle of attacks.

Table 3: Observations for 2D airfoil

Velocity = 100 m/s				
α	CL (Experimental)	CL (Theory)	CD (Experimental)	CD (theory)
0	0.0001	0	0.015	0.02078
2.5	0.32	0.3499	0.018	0.02436
5	0.551	0.6194	0.019	0.02413
10	0.79	0.8198	0.075	0.0758

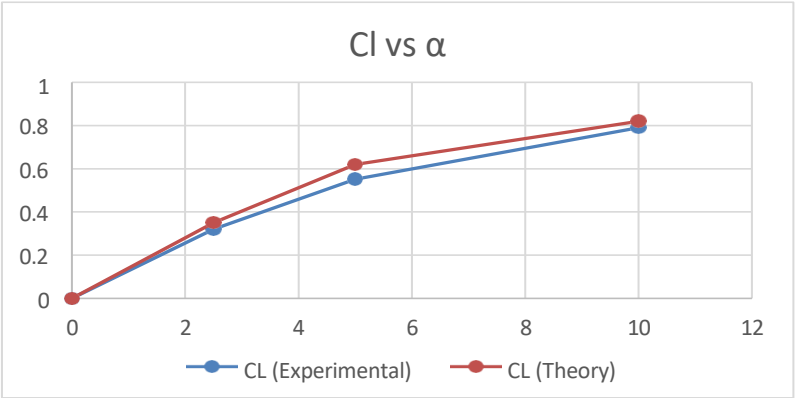

Fig 38: C_L vs α

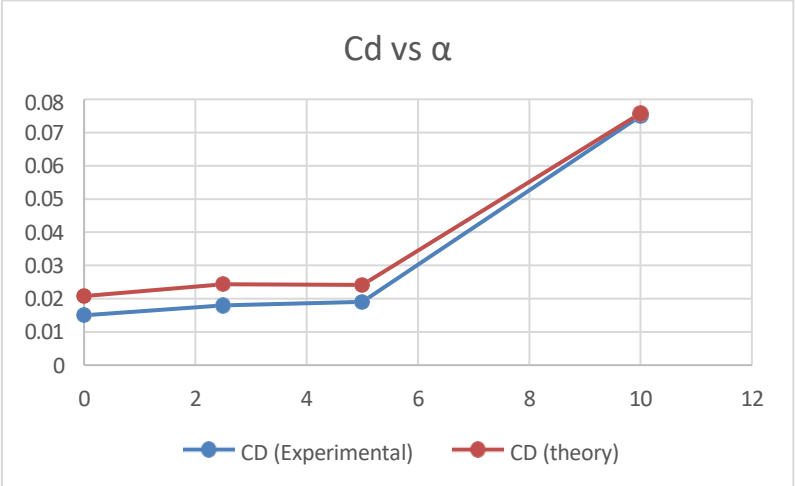

Fig 39: C_D vs α

RESULT AND DISCUSSION

The flow over a cropped delta wing is analyzed for subsonic speed of velocity=100mps.

The pressure distribution is a crucial factor in determining the wing's ability to produce lift with the least amount of resistance as it illustrates the air's interaction o f a i r with the wing. Both the upper and lower surface pressure plots roughly coincide at a 0° angle of attack (AOA), which is a condition when the wing is parallel to the approaching airflow and the forces acting on the wing are distributed symmetrically. At a 0° angle of attack (AOA), the pressure contours at lower speeds show a symmetric flow pattern. This symmetry is essential because it depicts an aerodynamically balanced condition in which the forces operating on the wing are dispersed equally. Variations in lift and drag result from changes in the pressure distribution brought about by an increase in angle of attack. The spanwise pressure distribution was also calculated for different values of x and was verified by the experimental values given in Fundamentals of Aerodynamics by J D Anderson Jr. It implies that the CFD Simulation results agree with accepted aerodynamic theories.

International Journal of Engineering Research & Technology (IJERT)
ISSN: 2278-0181
Vol. 14 Issue 02, February-2025

There is a noticeable shift in the pressure distribution as the angle of attack increases. In comparison to the bottom surface, the pressure on the wing's upper surface decreases. This change improves lift generation by increasing the pressure difference. It can be seen that for lower angle of attack such as 5 and 10 deg, higher pressure areas are visible at the tip chord of the wing, whereas as the angle of attack increase, it starts disappearing and prominent difference on upper and lower surface is observed.

The visualisation of streamlines and pathlines was done to obtain deeper insights into different elements of the flow behaviour, in particular the dynamics of leading edge vortices and the lines of attachment and dissociation, streamlines and pathlines are depicted. Streamlines show areas of high and low pressure and show how air flows across the wing's surface. The production of leading edge vortices (LEVs), which is a feature of flow over a delta awing and helps in increasing lift, particularly at higher angles of attack, may be seen in the streamlines of a delta wing. It is observed that at 0 deg AOA, very weak vortices are formed. As the AOA increases, it is observed that the flow is more disturbed and stronger and bigger vortices are formed. At lower AOA, vortices are smaller in size and are formed very near to the tip, whereas as AOA increases, they increase in size.

Pathlines, on the other hand, show the course that individual fluid particles would follow as they pass through the flow field over time. By demonstrating how air particles arrive and depart various areas around the wing, pathline analysis sheds light on the transient behaviour of flow. This knowledge is especially crucial for comprehending flow separation, which happens when the smooth flow of air separates from the wing surface. Separation lines show the point at which the flow separates, increasing drag and decreasing lift. At lower AOA, it is seen that the flow remains comparatively undisturbed and higher values are seen at just the ending of the wing. As AOA increases, the area of higher values increases and it can be observed that the flow has become more disturbed.

This stage entailed modelling the airfoil's aerodynamic properties in a reduced setting, enabling a concentrated analysis of lift and drag behaviours without the complications brought on by three-dimensional effects. Subsequently, the outcomes of this 2D analysis were compared to established data. A strong validation of the CFD analysis was provided by the near match between the computational results and the published data It was noted that the Lift Coefficient obtained through computational analysis was less than the 2D airfoil's quoted value in the literature. Simultaneously, the Drag Coefficient was examined. The numbers derived from computational techniques were carefully cross-checked against online data.

CONCLUSION

A numerical study of aerodynamic characteristics, namely lift and drag coefficients and pressure distribution, over a 3-D cropped delta wing of the kind used in Tejas fighter aircraft has been carried out. The computational results are in line with the expected theoretical results. The technique has been validated by first performing the 2-D simulation. With the confidence gained through this analysis, the authors plan to take up similar study on a complete aircraft.

REFERENCES

[1] http://airfoiltools.com/airfoil/details?airfoil=n 0012- il
[2] Korkmaz, S., Ertunc, H. M., & Altintas, O. (2017). Aerodynamic performance of compound delta wings in low-speed wind tunnel experiments. Journal of Aircraft, 54(3), 1154-1162.
[3] Numerical Analysis of Flow Field over Compound Delta Wing at Subsonic and Supersonic Speeds by Gaurav Sharma, Mohd Naimuddin, Gaurav Chopra, Jayanta Sinha and Gaga
[4] Analysis of Vortex dominated flow field over a delta wing at transonic speed by T. Di. Fabbio, E. Tangermann and M. Klein
[5] Flow Analysis on Delta Wing- A review by Y.D. Dwivedi, C. Navaneetha and Vasishta Bhargava
[6] Experimental and Computational Study on Compound Delta Wing by Gaurav Sharma, Mohd Naimuddin, Gaurav Chopra, Jayanta Sinha and Gaga
[7] Matak L., Krajček Nikolić K.: CFD Analysis of F- 16 Wing Airfoil Aerodynamics in Supersonic Flow